Functional connectivity patterns of normal human swallowing: difference among various viscosity swallows in normal and chin-tuck head positions

Iva Jestrović* James L. Coyle† Subashan Perera‡ Ervin Sejdić

Abstract

Consuming thicker fluids and swallowing in the chin-tuck position has been shown to be advantageous for some patients with neurogenic dysphagia who aspirate due to various causes. The anatomical changes caused by these therapeutic techniques are well known, but it is unclear whether these changes alter the cerebral processing of swallow-related sensorimotor activity. We sought to investigate the effect of increased fluid viscosity and chin-down posture during swallowing on brain networks. 55 healthy adults performed water, nectar-thick, and honey thick liquid swallows in the neutral and chin-tuck positions while EEG signals were recorded. After pre-processing of the EEG timeseries, the time-frequency based synchrony measure was used for forming the brain networks to investigate whether there were differences among the brain networks between the swallowing of different fluid viscosities and swallowing in different head positions. We also investigated whether swallowing under various conditions exhibit small-world properties. Results showed that fluid viscosity affects the brain network in the *Delta*, *Theta*, *Alpha*, *Beta*, and *Gamma* frequency bands and that swallowing in the chin-tuck head position affects brain networks in the Alpha, Beta, and Gamma frequency bands. In addition, we showed that swallowing in all tested conditions exhibited small-world properties. Therefore, fluid viscosity and head positions should be considered in future swallowing EEG investigations.

Keywords: Dysphagia, swallowing, brain networks, EEG, fluid viscosity.

*Iva Jestrović and Ervin Sejdić are with Department of Electrical and Computer Engineering, Swanson School of Engineering, University of Pittsburgh, Pittsburgh, PA, USA. E-mails: ivj2@pitt.edu, esejdic@ieee.org. Ervin Sejdić is the corresponding author.

†James L. Coyle is with the Department of Communication Science and Disorders, School of Health and Rehabilitation Sciences, University of Pittsburgh, Pittsburgh, PA, USA. E-mail: jcoyle@pitt.edu

‡Subashan Perera is with the Department of Medicine, Division of Geratric Medicine, School of Medicine, University of Pittsburgh, Pittsburgh, PA, USA. E-mail: ksp9@pitt.edu

1 Introduction

1.1 Swallowing and swallowing difficulties

Deglutition (i.e., swallowing) is one of the most complex human functions as it involves the activation of several brain and brainstem regions, as well as peripheral structures including head and neck muscles (Ertekin and Aydogdu, 2003; Stevenson and Allaire, 1991). This process of food transportation from the oral cavity via the pharynx and esophagus to the stomach is divided into four phases (Dodds, 1989). The first swallowing phase, the oral preparatory phase, is entirely voluntary, while the second, the oral transit phase, is initiated voluntarily and completed involuntarily. During the oral preparatory phase, food is formed into a swallowable bolus by chewing and mixing with saliva. At the same time sensory information is delivered to the brainstem and cortical centers (Hughes et al., 1987). Meanwhile, lingual and palatal musculature contains the bolus within the oral cavity, preventing inadvertent gravity-dependent flow of material from the oral cavity into the pharynx, where the airway remains unprotected (Saitoh et al., 2007). Depending on the information collected by sensory receptors about the food or liquid being prepared, these receptors generate signals that stimulate activation of salivatory nuclei in the pons and medulla to produce salivation in the oral cavity and masticatory motor activity in the head and neck. Furthermore, the signals generated by the sensory receptors elicit limbic-mediated emotions related to the act of feeding, and this cumulative sensory afferent information is processed in the pontomedullary swallowing centers in preparation for the subsequent phases of swallowing (Miller, 1986). During the oral transit phase, intrabolus pressure generated by the tongue propels the bolus posteriorly by compressing the bolus against the palate, while the posterior linguapalatal valve is opened to enable transfer of the bolus to the pharynx (Nicosia and Robbins, 2001; Miller and Watkin, 1996). In healthy young individuals, the onset of the next phase, the pharyngeal phase, begins before the leading edge (head) of the bolus enters the pharyngeal cavity, while in older individuals, pharyngeal motor activity is observed after the bolus head enters the pharynx (Hughes et al., 1987). The duration between the entrance of the bolus head into the pharynx and the onset of pharyngeal motor activity is referred to as the duration of stage transition (Kempster, 1992).Throughout these events, oropharyngeal receptors continue to transmit information about the size, shape, temperature, taste, and speed of motion of the food or liquids being processed. After processing, this information is received by the trigeminal and solitary nuclei and their associated reticular formation. A motor plan is produced by the swallowing central pattern generator and the muscles involved in the pharyngeal phase are automatically activated (Miller, 1999). The third phase, the pharyngeal phase, is a nearly entirely

combination of voluntary and involuntary actions and involves numerous biomechanical events that continuously transfer intrabolus pressure to the inferior pharynx, inhibit resting closure pressure of the upper esophageal sphincter (UES), displace the unprotected airway out of the path of the oncoming bolus, cover the inlet to the airway, seal the superior nasopharynx at the velopharyngeal port, and apply the necessary traction forces on the UES to enable adequate duration and diameter of opening for complete bolus clearance into the digestive system. The fourth phase, the esophageal phase, is a totally involuntary process mediated by vagal efferents and the somewhat internal esophageal nervous system that produces propulsive, sequential superior to inferior motor activity propelling the bolus toward the lower esophageal sphincter, which then momentarily relaxes and enables clearance into the stomach (Goyal et al., 2001). Historically, it was believed that only brainstem centers were responsible for controlling swallowing; however, later studies emphasized the importance of the cerebral cortex during swallowing (Martin and Sessle, 1993). Other parts of the brain which that later demonstrated activity during swallowing include: the faciale areas of the sensorimotor cortices, the premotor cortex, the anterior cingulate cortex, the insular cortex, the frontal operculum, the cerebellum, etc. (Hamdy et al., 1999a,b; Martin et al., 2001; Kern et al., 2001; Mosier and Bereznaya, 2001; Zald and Pardo, 1999).

There are numerous supra and infratentorial regions, including a pontomedullary "swallowing cente" which are activated during swallowing, and others which, when directly stimulated, produce facial, lingual and mandibular movements. And the combined mastication-swallowing patterns can be elicited through electrical stimulation. Prefrontal microeletrode stimulation has been show to produce specific contractions of muscles responsible for movement of these structures, while more current delivered through larger electrodes has been shown to produce the pharyngeal swallow response (Miller, 1986). Likewise, stimulation of corticobulbar and subthalamic regions adjacent to the substantia nigra and midbrain reticular formation regions have been shown to also elicit a masticatory-swallow response. Early research into these deep brain regions and their relationship to swallowing suggests that autonomic and other visceral and somatic responses integrate with one another and summate to produce the reflexive swallow as well as esophageal activity Bieger (1993). Therefore these higher level centers appear to be involved in acquisition of feeding and swallowing behaviors and related motor learning. However the activation and propagation of the coordinated swallow response is strongly mediated by infratentorial, brainstem regions. General sensory input through trigeminal, glossopharyngeal and vagal nerves, and gustatory input through facial and glossopharyngeal nerves from the periphery, deliver the necessary kinesthetic, taste, proprioceptive and tactile input to the solitary nucleus that summate in the swallowing center Stimulation of pon-

tine areas adjacent to the trigeminal motor nucleus also evoke mastication and swallowing while destruction of the dorsolateral medulla, as seen in posterior inferior cerebellar artery syndromes like the lateral medullary or Wallenberg syndrome, is well-known to produce the clinical syndrome of dysphagia characterized by an absent pharyngeal response, failure of inhibition cricopharyngeal (upper esophageal sphincter) tonic closure, and pharyngeal and laryngeal paralysis, with preserved buccofacial and masticatory behavior. This region, containing portions of the reticular formation and adjacent nucleus and tractus solitarius (the principal sensory nucleus receiving vagal general afferent and special sensory information from the oropharyngeal mechanism) and nucleus ambiguus (the principal motor nucleus activating the pharyngeal, laryngeal and esophageal structures innervated by the 9th and 10th cranial nerves), and surrounding structures, has been referred to as the medullary swallowing center (Sang and Goyal, 2001) . Interestingly, unilateral dorsolateral medullary damage has been shown to produce contralateral sensorimotor impairments and bilateral swallowing disconnection syndromes (Aydogdu et al., 2001).

Swallowing difficulties (i.e., dysphagia) may occur for a wide range of reasons, the most common of which includes neurological conditions, such as stroke (Gottlieb et al., 1996), brain injuries (Lazarus and Logemann, 1987), cerebral palsy (Rogers et al., 1994), Parkinson's and other neurodegenerative diseases (Murray, 1999). Dysphagic patients have a high risk of developing other medical conditions (i.e., dehydration (Smithard et al., 1996), malnutrition Foley et al. (2009), failure of the immune system (Curran and Groher, 1990), and respiratory infections (Marik and Kaplan, 2003)), which can lead to hospitalization and to death. One of the common techniques for treating dysphagia is by changing the patient's diet. Studies show that the alteration of the texture and other sensory properties of certain foods and liquids can make swallowing easier for patients with certain impairments in bolus propulsion, airway protection, and kinematics of aerodigestive tract structures responsible for clearance into the esophagus (Clavé et al., 2006). Increasing bolus viscosity not only makes swallowing easier for some patients, but also reduces the risk of aspiration in many patients who aspirate ordinary thin liquids due to specific swallowing biomechanical swallowing impairments (Cook and Kahrilas, 1999). One large randomized controlled trial reported that during a videofluoroscopic examination, the use of thickened liquids in 711 individuals with Parkinson's disease who aspirate thin liquids and/or dementia eliminated aspiration by 37% when using nectar-thick liquids (300 Centipoise), and by 47% for honey-thick liquids (3,000 Centipoise) (Logemann et al., 2008). Another common method for treating dysphagia is by incorporating postural alterations in head and neck position during swallowing. Swallowing in the chin-tuck head position has been very helpful in protecting airways in many patients who aspirate while swallowing (Lewin

et al., 2001; Logemann, 1998; Bülow et al., 1999). In this position, the patient flexes the head on the neck to bring the chin close to the neck while swallowing. In the first investigation of this compensatory technique, it was reported that this posture eliminated aspiration in 50% of patient with stroke who aspirated thin liquids on the videofluoroscopic swallow examination (Shanahan et al., 1993). Since their initial discovery as aspiration-reducing interventions, increasing the bolus viscosity and swallowing in the chin-tuck position have become widely accepted as methods for treating thin-liquid aspiration in patients with neurological and other dysphagia-producing conditions. Even though studies provided physiological explanations of the peripheral effects of these two therapeutic techniques on protecting airways, it remains unknown whether maneuvers such as the chin-tuck position and increased bolus viscosity affect the central nervous system and on the brain activity during swallowing. Elucidation of the possible central effects of these and other dysphagia interventions can lead to a better understanding of the central substrates of swallowing and potentially lead to a wider variety of effective swallowing therapeutic techniques. As a result, analysis of brain activity during various swallowing conditions provides an additional route of investigation that warrants attention.

1.2 Brain network formed with EEG

The electroencephalography (EEG), is one of the techniques used for investigating brain activity during swallowing in different condition as well as for investigating motor imagery of swallow (Huckabee et al., 2003; Jestrović et al., 2014; Satow et al., 2004; Kober and Wood, 2014; Jestrović et al., 2015; Kober et al., 2015; Yang et al., 2014, 2016; Jestrović et al., 2015). Traditionally, EEG were very useful for gaining information about which parts of the brain are involved in the swallowing task. Besides identification of the brain regions involved in swallowing, EEG also enables the investigation of relationships and interactions among brain regions during swallowing. The idea of brain connectivity (i.e., how brain regions communicate between each other) during swallowing should provide understanding of the brain organization, which is beyond the simple identification of the brain region involved in this activity. The graph theoretical approach is one of the methods for analysis of the functional interactions among the brain regions. Graph theory mathematically describes the relationships between vertices (nodes) of the graph. This approach has been widely used in human and animal neuroscience studies, as it provides easy analysis of the functional connectivity of brain networks (Eguiluz et al., 2005; Kaiser and Hilgetag, 2004; Micheloyannis et al., 2006; Sporns and Zwi, 2004). Therefore, we believe that this method could

be useful for investigating the functional connectivity of brain networks during swallowing.

In the brain networks formed with the EEG time series, vertices denote the EEG electrodes, while edges describe synchronization between signals from each pair of electrodes. Depending on the position of the vertices and the strength of the edges between them, the brain network will have certain architectural properties. Architectural properties of the brain network formed from the EEG time series recorded during the swallowing will describe if the neural organization of this activity is more regular or more random. If the brain network formed during swallowing is regular, it will be characterized by strong local clustering and a long path length connecting any two brain regions. On the other hand, if the brain network formed during the swallowing is random, it will have weak local clustering but short path length between the brain regions. Studies show that optimal architectural organization of the brain network has so-called small-world properties (Watts and Strogatz, 1998). A network with small-world properties has strong local clustering and short path length between brain regions. It has been shown that brain networks with small-world properties provide optimal organization with the more efficient communication between different brain regions (Lago-Fernández et al., 2000; Masuda and Aihara, 2004). Also, higher small-world index implies more efficient communication and a better organization within a brain network (Douw et al., 2011). Understanding optimal brain organization during swallowing, as well as understanding changes in the neural reorganization due to cerebral injuries that cause dysphagia could potentially lead to better rehabilitation strategies. Thus, investigation of the small-worldness of the brain network during various swallows is of particular interest to us. Also, the difference in architectural properties between networks that are formed during swallowing from various conditions could provide important insights into the core of human brain function during swallowing.

1.3 Hypothesis

We hypothesized that the brain network is different among swallows of various fluid viscosities, as well as between swallowing in the neutral and chin-tuck head positions. We also hypothesized that the brain activity occurring during swallowing of various fluid viscosities has would exhibit small-world properties in both neutral and chin-tuck head positions. Investigation of brain activity during swallowing of thicker liquids and during swallowing in the chin-tuck head position could explain whether better swallowing control during these two therapeutic techniques is simply due to anatomical changes in the pharynx, or rather due to changes in sensory and motor activation

controlled by brain. Brain damage induced by neurological disorders responsible for dysphagia may also affect the brain regions involved in swallowing control during these two therapeutic techniques (e.g., brain regions responsible for sensation during swallowing of the higher-viscosity fluids, or brain regions responsible for motor activity during swallowing in different head positions). Characterizing the brain network during these therapeutic techniques could potentially explain why they are only partially efficient in preventing aspiration. In addition, we analyze whether networks formed during swallowing with thicker liquids have a higher small-world organization than the networks formed during swallowing of the thinner liquids. Also, we want to know if small-world organization is higher for the networks during swallowing in chin-tuck position in comparison with the neutral position.

2 Results

The results of the network measures are presented as a mean value ± standard deviation, as a function of percent of network connections. For analyzing the pairwise comparison among various swallowing conditions, we considered in neutral head position 245 water (thin liquid) swallows, 233 nectar-thick liquid swallows, and 228 honey-thick liquid swallows, while in the chin-tuck head position, we analyzed 229 water swallows, 216 nectar swallows, and 217 honey swallows.

Figure 1 contains five figures. Each figure summarizes the mean value for the clustering coefficient as a function of connection densities (i.e., from 5% to 100%) in one of the five EEG frequency bands. Each colored line indicates a different bolus viscosity. Pairwise comparison between nectar-thick and honey-thick swallows did not exhibit significant differences in *Gamma* frequency band for the viscosity dependence alone, nor for the multivariable dependence of network parameters on head position, viscosity and sex ($p > 0.05$). However, nectar-thick swallows had a significantly higher clustering coefficient than water swallows in the *Delta* (5% - 65%, moderate effect size: 0.3 - 0.6), *Theta* (15% - 90%, moderate effect size: 0.3 - 0.56), *Alpha* (5% - 90%, moderate effect size: 0.3 - 0.54), *Beta* (5%, 20% - 45%, 55%, small effect size: 0.2 - 0.35), and *Gamma* (20% - 35%, moderate effect size: 0.3 - 0.34) ranges ($p < 0.0167$) for the viscosity dependence alone as well as for the multivariable dependence ($p < 0.05$). Also, honey-thick swallows had a significantly higher clustering coefficient than water swallows in all five frequency ranges for the viscosity dependence alone (*Delta* (5% - 25%, large effect size: 0.56 - 0.84), *Theta* (10%, 15%, moderate effect size: 0.36 - 0.47), *Alpha* (10%, 15%, moderate effect size: 0.43 - 0.53), *Beta* (5% - 20%, 40% - 85%, moderate effect size: 0.33 - 0.56), and *Gamma* (5% - 20%, 35% - 75% , moderate effect size: 0.3 - 0.51))

Table 1: Summarized statistically significant results for the clustering coefficient between different pairwise comparisons, where W-N is a pairwise comparison between water and nectar, W-H is a pairwise comparison between water and honey, and N-H is a pairwise comparison between nectar and honey. The dot denotes a significant statistical difference.

Density	*Delata*			*Theta*			*Alpha*			*Beta*			*Gamma*		
	W-N	W-H	N-H	W-N	W-H	N-H	W-N	W-H	N-H	W-N	W-H	N-H	W-N	W-H	N-H
5%	•	•					•			•	•			•	
10%	•	•			•		•	•			•			•	
15%	•	•		•	•		•	•			•			•	
20%	•	•		•			•			•	•		•	•	
25%	•	•		•		•	•		•	•			•		
30%	•			•		•	•		•	•			•		
35%	•			•		•	•		•	•			•	•	
40%	•		•	•		•	•		•	•	•			•	
45%	•		•	•		•	•		•	•	•			•	
50%	•		•	•		•	•		•		•			•	
55%	•		•	•		•	•		•	•	•			•	
60%	•		•	•		•	•		•		•			•	
65%	•		•	•			•		•		•			•	
70%			•	•			•		•		•			•	
75%			•	•			•		•		•			•	
80%				•			•				•				
85%				•			•				•				
90%				•			•								
95%							•								
100%															

and for the multivariable dependence (*Delta* (5% - 25%), *Theta* (10%, 15%), *Alpha* (10%, 15%), *Beta* (5% - 15%, 40% - 85%), and *Gamma* (10% - 20%, 40% - 75%)) ($p < 0.05$). Furthermore, honey-thick swallows had a significantly higher clustering coefficient than nectar-thick swallows in the *Delta* (40% - 75%, moderate effect size: 0.45 - 0.56), *Theta* (25% - 60%, moderate effect size: 0.45 - 0.56), *Alpha* (25% - 75%, moderate effect size: 0.39 - 0.58), and *Beta* (25%, 30%, moderate effect size: 0.39 - 0.43) ranges for the viscosity dependence alone, and in the *Delta* (40% - 70%), *Theta* (45%), and *Alpha* (25% - 75%) ranges for the multivariable dependence ($p < 0.05$). The results for the significant statistical differences for the clustering coefficients are also summarized in the Table 1

Figure 2 contains five figures. Each figure summarizes the mean value for the characteristic path length as a function of connection densities (i.e., from 5% to 100%) in one of the five EEG frequency bands. Each colored line indicates a different bolus viscosity. Pairwise comparison between nectar-thick and honey-thick swallows did not exhibit significant differences in the *Beta* and *Gamma* frequency bands for the viscosity dependence alone, nor for the multivariable dependence of network parameters on head position, viscosity and sex ($p > 0.05$). However, water swallows had a significantly higher characteristic path length than nectar-thick swallows in the *Delta* (20% - 40%, moderate effect size: 0.31 - 0.34), *Theta* (15% - 50%, moderate effect size: 0.31 - 0.47), *Alpha* (20% - 50%, moderate effect size: 0.37 - 0.47), *Beta* (35% - 50%, moderate effect size: 0.34 - 0.44), and *Gamma* (40% - 50%, moderate effect size: 0.33 - 0.36) ranges for the viscosity dependence alone, and in the *Delta* (20%), *Theta* (20% - 50%), *Alpha* (20% - 50%), *Beta* (35% - 55%), and *Gamma* (40% - 50%) ranges for the multivariable dependence ($p > 0.05$). Also, water swallows had a significantly higher characteristic path length than honey-thick swallows in all five frequency ranges for the viscosity dependence alone (*Delta* (5% - 25%, 35% - 75%), *Theta* (10%, 15%, 30% - 50%), *Alpha* (5% - 15%, 35% - 70%), *Beta* (15%, 20%, 30% - 60%), and *Gamma* (20%, 25%, 40% - 55%)) and for the multivariable dependence (*Delta* (5% - 25%, 35% - 75%, moderate effect size: 0.35 - 0.49), *Theta* (10%, 15%, 30% - 50%, high effect size: 0.61 - 0.8), *Alpha* (5% - 20%, 30% - 70%, moderate effect size: 0.38 - 0.45), *Beta* (15%, 20%, 30% - 60%, moderate effect size: 0.31 - 0.47), and *Gamma* (20%, 25%, 40% - 55%, moderate effect size: 0.31 - 0.51)) ($p < 0.05$). Furthermore, nectar-thick swallows had a significantly higher characteristic path length than honey-thick swallows in the *Delta* (30% - 45%, moderate effect size: 0.32 - 0.41), *Theta* (20% - 25%, moderate effect size: 0.33 - 0.42), and *Alpha* (20% - 25%, moderate effect size: 0.32) ranges for the viscosity dependence alone, and in the *Delta* (30%), *Theta* (20% - 25%), and *Alpha* (20% - 25%) ranges for the multivariable dependence ($p < 0.05$). The results for the significant statistical differences for the characteristic path length are also summarized in the Table 2

Figure 3 contains five figures. Each figure summarizes the mean value for the small-worldness as a function of connection densities (i.e., from 5% to 100%) in one of the five EEG frequency bands . Each colored line indicates a different bolus viscosity. Pairwise comparison between nectar-thick and honey-thick swallows did not exhibit significant differences in the *Theta*, *Alpha*, *Beta*, and *Gamma* frequency bands for the viscosity dependence alone, nor for the multivariable dependence of network parameters on head position, viscosity and sex ($p > 0.05$). However, nectar-thick swallows had a significantly higher small-worldness than water swallows in the *Delta* (15% - 60%), *Theta* (15% - 85%), *Alpha* (5% - 85%), *Beta* (5% - 65%), and *Gamma* (15%, 35% - 50%, 60%) ranges for the

Table 2: A summary of statistically significant results for the characteristic path length between different pairwise comparisons, where W-N is a pairwise comparison between water and nectar, W-H is a pairwise comparison between water and honey, and N-H is a pairwise comparison between nectar and honey. The dot denotes a statistically significant difference.

Density	*Delata*			*Theta*			*Alpha*			*Beta*			*Gamma*		
	W-N	W-H	N-H	W-N	W-H	N-H	W-N	W-H	N-H	W-N	W-H	N-H	W-N	W-H	N-H
5%		•						•							
10%		•			•			•							
15%		•		•	•			•			•				
20%	•	•		•		•	•		•		•			•	
25%	•	•		•		•	•		•					•	
30%	•		•	•	•		•				•				
35%	•	•	•	•	•		•	•		•	•				
40%	•	•	•	•	•		•	•		•	•		•	•	
45%		•	•	•	•		•	•		•	•		•	•	
50%		•		•	•		•	•		•	•		•	•	
55%		•						•			•			•	
60%		•						•			•				
65%		•						•							
70%		•						•							
75%		•													
80%															
85%															
90%															
95%															
100%															

viscosity dependence alone, as well as for the multivariable dependence ($p > 0.05$). Also, honey-thick swallows had a significantly higher characteristic path length than water swallows in all five frequency ranges for the viscosity dependence alone (*Delta* (10% - 20%, 45% - 80%, moderate effect size: 0.31 - 0.53), *Theta* (5%, 10%, 20%, 25%, 50% - 85%, moderate effect size: 0.33 - 0.44), *Alpha* (5% - 20%, 70% - 80%, moderate effect size: 0.31 - 0.41), *Beta* (5% - 80%, moderate effect size: 0.35 - 0.49), and *Gamma* (5% - 65%, small effect size: 0.19 - 0.3)) and for the multivariable dependence (*Delta* (10% - 20%, 50% - 80%), *Theta* (5%, 10%, 20%, 25%, 50% - 85%), *Alpha* (5% - 20%, 70% - 80%), *Beta* (5% - 80%), and *Gamma* (5% - 65%)) ($p < 0.05$). Furthermore, honey-thick swallows had a significantly higher small-worldness than nectar-thick swallows in the *Delta* (20% - 55%, moderate effect size: 0.32 - 0.35) range for the viscosity dependence alone, and in the *Delta* (30% - 40%) range for the multivariable dependence ($p < 0.05$).

We also compared extracted features between different head positions. Small-worldness did not show statistical difference between two head positions ($p > 0.05$). Also, characteristic path length and clustering coefficient exhibited no significant difference between swallowing in neutral and chin-tuck head positions in the *Delta* and *Theta* frequency ranges ($p > 0.05$). However, swallowing in chin-tuck head position had higher clustering coefficient than swallowing in neutral head position in the *Alpha* (25% - 85% moderate effect size: 0.31 - 0.44), *Beta* (5%, 10%, 20% - 90% moderate effect size: 0.39 - 0.55), and *Gamma* (5%, 10%, 25%, 30%, 50% -80% moderate effect size: 0.32 - 0.41) frequency ranges for the head position dependence alone, and in *Alpha* (5%, 25% - 85%), *Beta* (5%, 10%, 20% - 90%), and *Gamma* (5%, 10%, 25%, 30%, 50% -80%) ($p < 0.05$). Also, swallowing in chin-tuck head position had smaller characteristic path length than swallowing in neutral head position in the *Alpha* (10$ - 20%, 45% - 55%, 70% moderate effect size: 0.37 - 0.46), *Beta* (10%, 70% - 80% moderate effect size: 0.32 - 0.395), and *Gamma* (5%, 10%, 75% moderate effect size: 0.41 - 0.52) frequency ranges for the head position dependence alone, and in the *Alpha* (10$ - 20%, 45% - 55%, 70%), *Beta* (10%, 70% - 80%), and *Gamma* (10%, 75%) ($p < 0.05$). The results for the significant statistical differences for the small-worldness are also summarized in the Table 3

In addition Figure 4 represents brain networks of the various conditions. The brain networks are formed as mean value of networks across the swallows in various conditions, and thresholded such that we kept 25% of the strongest connections. It can be seen a strong interconnection between the right and left hemispheres in the frontal regions, as well within right side of the posterior frontal and parietal regions. Also, there are no significant changes in the localization of interconnections among various conditions.

Table 3: Statistically different small-worldness values for pairwise comparisons, where W-N is a pairwise comparison between water and nectar, W-H is a pairwise comparison between water and honey, and N-H is a pairwise comparison between nectar and honey. Dots denote statistically different cases.

Density	*Delata*			*Theta*			*Alpha*			*Beta*			*Gamma*		
	W-N	W-H	N-H	W-N	W-H	N-H	W-N	W-H	N-H	W-N	W-H	N-H	W-N	W-H	N-H
5%					•		•	•		•	•			•	
10%		•			•		•	•		•	•			•	
15%	•	•		•			•	•		•	•		•	•	
20%	•	•	•	•	•		•	•		•	•			•	
25%	•		•	•	•		•			•	•			•	
30%	•		•	•			•			•	•			•	
35%	•		•	•			•			•	•		•	•	
40%	•		•	•			•			•	•		•	•	
45%	•	•	•	•			•			•	•		•	•	
50%	•	•	•	•	•		•			•	•		•	•	
55%	•	•	•	•	•		•			•	•			•	
60%	•	•		•	•		•			•	•		•	•	
65%		•		•	•		•			•	•			•	
70%		•		•	•		•	•			•				
75%		•		•	•		•	•			•				
80%		•		•	•		•	•			•				
85%				•	•		•								
90%															
95%															
100%															

3 Discussion

Our hypothesis, that swallowing of various fluid viscosities has small world properties in the neutral and chin-tuck head positions was supported by our results. Our other hypothesis that the brain network is different in the swallowing of various fluid viscosities, as well as between swallowing in the neutral and chin-tuck head positions, was also supported by our results.

It has been reported that the *Delta*, *Theta*, and *Alpha* frequency bands exhibit changes in activation during sensory stimulation (Baslar and Stampfer, 1985; Yordanova et al., 2002; Basar et al., 1991). Swallowing is a complex process that involves different types of sensory stimulation such as smell, taste, temperature, and touch in the oral areas. Stimuli that are used in the study are characterized by different viscosities (i.e., water, nectar-thick, and honey-thick) and different tastes (i.e., water and apple juice) that affect the sensory receptors responsible for touch and the sensory receptors responsible for taste. In the previous studies, changes in the *Theta* (Stacher et al., 1979; Lorig and Schwartz, 1988; Yagyu et al., 1998), *Delta* (Yagyu et al., 1998), and *Alpha* (Klemm et al., 1992; Lorig et al., 1991) frequency bands during these sensory components of the swallowing were reported. Thus, changes in these three frequency bands (*Delta*, *Theta*, and *Alpha*) could be attributed to the evoked sensation that stimuli from the study produced.

Besides activation during sensory stimulation, it has been reported that the *Alpha* frequency band is also associated with inhibition control (Herrmann et al., 2004; Mathewson et al., 2011; Sauseng et al., 2005). Our results showed a higher clustering coefficient in the *Alpha* frequency band than for the swallowing in the chin-tuck head position. Swallowing in the chin-tuck position exhibits changes in the pharyngeal dimensions, owing to an unnatural execution of performing the swallowing act (Welch et al., 1993). As a consequence, swallowing in the chin-tuck position exhibits reduced muscular recruitment in the pharyngeal dimensions when compared with swallowing in neutral head position (Balou et al., 2014). Therefore, we can attribute changes in the alpha frequency band to the inhibition which is responsible for the reduced muscular recruitment that swallowing in chin-tuck head position produces.

Studies investigating cortico-muscular synchronization suggested that the *Beta* EEG frequency band is correlated to attention during certain sensorimotor tasks (Sanes and Donoghue, 1993; Kristeva-Feige et al., 1993; Brown and Marsden, 1998). Even though consuming thicker liquids and using the chin-tuck postural technique are considered comfortable therapeutic techniques for a patient, swallowing under these conditions is not natural. Thus, these swallows will require more of the subject's attention and a higher awareness of the swallowing task. Therefore, changes in

the *Beta* EEG frequency band during swallowing of thicker liquids and swallowing in the chin-tuck head position could be attributed to the reallocation of cognitive resources towards these otherwise relatively automatic sensorimotor tasks.

A number of studies have reported activation of the Gamma EEG frequency band during different muscular recruitment demands (Herrmann and Mecklinger, 2001; Niedermeyer and da Silva, 2005; Kristeva-Feige et al., 2002). During swallowing, the tongue imparts pressure on the hard palate to propel the bolus (Mcconnel, 1988; Shaker et al., 1988). Studies have demonstrated increased submental muscular activity when swallowing thicker liquids, which was associated higher pressure on the palate during oral propulsion (Reimers-Neils et al., 1994). Also, changes in pharyngeal dimensions during swallowing in the chin-tuck head position are associated with changes in the muscle recruitment involved in swallowing (Niedermeyer and da Silva, 2005; Bülow et al., 1999). Therefore, changes in the *Gamma* frequency band during the swallowing of thicker fluids and swallowing in the chin-tuck position could be attributed to changes in muscle recruitment during these two therapeutic techniques.

Significant differences for the small-world parameter have been found in the swallowing of fluids of various viscosity in the *Delta*, *Theta*, and *Alpha* bands. This means that the sensation evoked during swallowing of thicker liquids will have an important role in providing better communication between brain neurons. Also, significant differences for the small-world parameter have been found between swallowing in the normal and chin-tuck positions in the *Alpha*, *Beta*, and *Gamma* frequency bands. These results indicate that central nervous system resource reallocation, as well as changes in muscle recruitment, will be involved in providing better communication among the brain regions responsible for swallowing in the chin-tuck position.

Studies have shown that small-world properties correspond to easier communication between neighboring nodes as well as a more efficient communication between far apart regions (Lago-Fernández et al., 2000; Masuda and Aihara, 2004). A greater small-world parameter for both the swallowing of thicker liquids and for swallowing in the chin-tuck position indicates that there is a possibility that a greater functional connectivity in the brain network during these therapeutic techniques contributes to increased swallowing safety in some dysphagic patients. However, the specific physiologic abnormalities that are ameliorated or facilitated by these techniques are still not clearly understood. Therefore, in order to understand how greater neural organization contributes to better swallowing control during these therapeutic techniques, similar studies should be performed on those patients that benefit from these techniques.

Previously, it has been reported that most of the brain regions involved in the swallowing activity

are concentrated in the right and left hemispheres of the frontal brain regions (Luan et al., 2013). In addition, Martin et al. (2004) reported activation of the insula, paracentral lobule, and middle occipital gyrus in the right hemisphere during water swallowing. Stronger interconnections within right and left hemispheres in the frontal regions, and within right side of the posterior frontal and parietal regions that our results showed implies that localization of the stronger functional brain connectivity during swallowing overlaps with the brain regions which activation is more prominent during swallowing. This means that graph theory approach applied on high temporal resolution EEG signals during swallowing can capture not only what regions activate, but how strongly they connect with each other in the healthy system. In the future, this approach could help understanding brain organization in the people with neurogenic dysphagia by analyzing how these connections might differ after unilateral hemispheric damage.

A limitation of our study is that the bolus volume was not controlled. Thus, there is a possibility that bolus volume, which has been shown to influence peripheral kinematics, could affect the brain networks. Also, the order of consumed stimuli and the order of head position in this study was specified and not randomized (i.e., water first, nectar-thick second, honey-thick third), which also could have influenced our result. Another limitation is that swallowing components responsible for sensation such as: taste, shape, and speed of motion of the liquids being processed were not strictly controlled even though they can possibly influence results measurements. Lastly, EEG signals are very sensitive to the artifacts. The chin-tuck head posture typically introduces artifacts that are due to head movements. Even though ICA was used to reduce artificats, it is possible that some unwanted components were still present even after ICA pre-processing steps. The ICA algorithm relies on visually identifying artifacts, and this step is highly dependent on the experience of a human observer. Therefore, future investigations should include bolus size measurements, randomize the order of the administered stimuli, and also investigate separately the swallowing components that elicit sensation. Also, future investigation should design experiments to reduce artifacts in EEG signals.

4 Conclusion

In this study we have investigated differences in the brain network between swallowing of various fluid viscosities in the neutral and chin-tuck head positions. Swallowing EEG signals were collected from 55 healthy adults who performed five water swallows, five nectar-thick apple juice swallows, and five honey-thick apple juice swallows, in both the neutral and chin-tuck head positions. Our

results showed differences in the brain networks between swallowing of different stimuli for all frequency bands of interest (i.e., *Delta*, *Theta*, *Alpha*, *Beta*, and *Gamma*). Also, our results demonstrated difference between swallowing in the neutral and chin-tuck head positions for the *Alpha*, *Beta*, and *Gamma* frequency bands. Additionally, we showed that the functional brain network has small-world properties during swallowing for all investigated conditions.

5 Methods and materials

5.1 Data acquisition from participants

The study was approved by the Institutional Review Board at the University of Pittsburgh. 55 healthy people, aged from 18 to 65, participated in the data acquisition process. The average age of the participants' was 38.58, and standard deviation of the participants age was 14.84. All participants signed a consent form and provided information about age, gender, height, and weight.

EEG signals were measured with 64 EEG electrodes positioned according to the 10-20 international electrode system (Jasper, 1958), using the actiCAP active electrodes cap (BrainProducts, Germany). Signals were amplified with the actiCHamp amplifier (BrainProducts, Germany). The P1 electrode was chosen for EEG voltage potential reference. Impedance of all electrodes was below 15 kΩ. Data were saved on a computer using PyCorder acquisition software, which also provided a 10 kHz sampling frequency. In order to determine the start and stop points of each swallow, we recorded swallowing vibrations with the dual axis accelerometer (ADXL322, Analog Devices, Norwood, MA, USA), which was placed on the anterior side of the participant's neck with double sided tape. The accelerometer is powered with a 3V output power supply (1504 DC/AC Power Supply, B&K Precision Corporation, Yorba Linda, CA, USA). The signal is amplified 10 times by an amplifier (P55, Grass Technologies, Warwick, RI, USA), which also provided band-pass filtering from 0.1 to 3000Hz. The accelerometer axis were positioned in anterior-posterior and superior-inferior direction. Systems operated the LabView software package Signal Express(National Instruments, Austin, TX, USA), which provides a 40Hz.

After setting up all devices, participants were instructed to perform three different tasks in two head positions. They were first asked to keep their head in neutral position and to perform five water swallows, then five nectar-thick apple juice swallows (nectar-thick, Nestlé Health Care Inc., Florham Park, N.J.), and then five honey-thick apple juice swallows (honey-thick, Nestlé Health Care Inc., Florham Park, N.J.). Later, they were asked to repeat the same series of swallows

in the chin-tuck head position. The unit for measuring viscosity was centipoise (cP), where 1 cP corresponds to the viscosity of water. Nectar-thick apple juice with a viscosity of 150cP is considered as mildly thick, while honey-thick apple juice with a viscosity of 400cP is considered as moderately thick. All bolus stimuli were served chilled (3-5C) in separate cups, with approximately one bolus per cup. Since there are sex-related difference in comfortable bolus size (Adnerhill et al., 1989), the bolus volume was not measured, but participants were instructed to consume a bolus of comfortable volume.

5.2 Pre-processing steps

Swallowing vibrations were first downsampled to 10kHz. Next, signals were filtered in order to remove noise from device. For that purpose, the FIR filter was designed as described in (Sejdić et al., 2010), using 18 baseline recordings. Then low frequency components produced by head movements were removed (Sejdić et al., 2012). Also, signals were denoised with 10-level discrete wavelet decomposition using the discrete Meyer wavelet with soft-thresholding (Donoho, 1995). The fuzzy c-means algorithm proposed by Sejdić et al. (2009) was used for signal segmentation. This algorithm was designed for dual-axis accelerometry signals and has shown over 90% accuracy in segmenting individual swallows from the accelerometer signal. All segmentations demarkated by the algorithm were visually inspected. Incorrectly segmented swallows were segmented manually. Time points determined in this process were used for the segmentation of the EEG signals.

The EEG data was pre-processed with the EEGlab MATLAB toolbox (Delorme and Makeig, 2004). In the first pre-processing step, signals were downsampled to 256 Hz. Then, signals were band-pass filtered from 0.1 Hz to 100 Hz, with an elliptical IIR filter. In the third step, signals were filtered again with an elliptical notch filter with cut-off frequencies at 58 Hz and 62 Hz, in order to remove noise from the power supply. Next, we did baseline correction of the signal. Then, signals were segmented on separate swallows determined by accelerometer signal segmentation points. Approximate swallowing duration was between one and four seconds. In the last pre-processing steps, artifacts were removed using the Independent Component Analysis (ICA) (Hyvärinen and Oja, 2000) algorithm. All artifact rejections were performed manually by visual inspection of the EEG signals. The most common artifacts in the EEG signals are due to eye-blinks, eye-movements, head movement, or disconnection of the electrode. These types of artifact are most distinctly represented in the time domain, and thus, they are easy to recognize (Urigüen and Garcia-Zapirain, 2015). Previous studies showed that ICA is a convenient method for removing

artifacts from the EEG signals (Olbrich et al., 2011; Hoffmann and Falkenstein, 2008; Srivastava et al., 2005). Therefore, we used ICA for artifact removal in this study. Signals contaminated with artifacts which couldn't be removed were excluded from the study. Less then 5% of EEG data samples were excluded.

5.3 Network constructions

Since EEG signals during swallowing activity are non-stationary (Jestrović et al., 2014), the time-frequency based phase synchrony measure proposed by Aviyente et al. (2011) was used to form connectivity networks. The time-frequency based phase synchrony measure was applied on data filtered in several frequency bands of interest: *Delta* ($< 4Hz$), *Theta* ($4-7Hz$), *Alpha* ($8-15Hz$), *Beta* ($16-31Hz$), *Gamma* ($> 32Hz$).

5.3.1 Time-frequency based phase synchrony measure

Synchrony is usually used for determining functional connectivity between neural osculation of different brain regions. The simplest way to measure synchronization between two signals could be defined as the current phase of both signals in the frequency of interest. This phase could be extracted either with the Hilbert transform or with the complex wavelet transform. No matter which of these two methods is used, the goal is to represent the signal as:

$$X(t,\omega) = a(t)exp(j(\omega t + \phi(t))), \tag{1}$$

where $a(t)$ is the current amplitude, and $\phi(t)$ is the current phase of the signal. The relationship between the signals x and y in the time domain can be approximated as a difference in their phase:

$$\Phi_{xy}(t) = |n\phi_x(t) - m\phi_y(t)| \tag{2}$$

where n and m are ratios of the locking frequencies, and ϕ_x and ϕ_y are phases of the signals x and y respectively.

The Rihaczek time-frequency distribution gives the representation of the signal energy distribution in both the both time and frequency domain, and is defined as:

$$C(t,\omega) = \frac{1}{\sqrt{2\pi}}(s(t)S^*(\omega)e^{-j\omega t}) \tag{3}$$

where $S(\omega)$ is a Fourier transform of the signal. The problem with the Rihaczek distribution is that it contains cross-terms which can introduce unwanted artifacts. In order to overcome cross-terms, we derived an interference version of the Rihaczek distribution by applying a Choi-Williams

(CW) kernel function with $\phi(\theta,\tau) = exp(-(\theta\tau)^2/\sigma)$ (Choi and Williams, 1989) to the Rihaczek distribution. The derived result can be written as:

$$C(t,\omega) = \int\int e^{(-(\theta\tau)^2/\sigma)} e^{(j(\theta\tau)/2)} A(\theta,\tau) e^{-j(\theta t+\tau\omega)} d\tau d\theta \tag{4}$$

where the term $A(\theta,\tau) = \int s(u+(\tau/2))s^*(u-(\tau/2))e^{j\theta u}du$ is the ambiguity function of the original signal, and the term $e^{(j(\theta\tau)/2)}$ is the kernel corresponding to the Rihaczek distribution.

From the calculated reduced interference version of the Rihaczek distribution for each signal, we can calculate a phase difference between any two signals:

$$\Phi_{12}(t,\omega) = arg\left[\frac{C_1(t,\omega)C_2^*(t,\omega)}{|C_1(t,\omega)||C_2(t,\omega)|}\right] \tag{5}$$

The calculated values for the phase difference between the signals' pairs are used for calculating the phase locking value (PLV). PLV measures phase differences, and is defined as:

$$PLV(t,\omega) = \frac{1}{N}\left|\sum_{k=1}^{N} exp(j\Phi_{12}^k(t,\omega))\right| \tag{6}$$

where N is the number of trails. PVL has values in the range from 0 to 1. If the phase difference between signal pairs does not vary much between trials, PVL tends to be higher.

5.4 Network measures

The calculated PVL values will correspond to the strength of the connection between every pair of nodes, forming a weighted undirected connectivity network. Weighted undirected connectivity matrices are converted into binary undirected matrices. In the case of binary networks, a connection between node i and node j (a_{ij}) has either a value of 1 or 0; $a_{ij} = 1$ if the connection exists, or $a_{ij} = 0$ if there is no connection between the two nodes. Binary networks are formed by thresholding of weighted networks. For analysis of the difference between two networks, it is important that they have the same number of connections. Therefore, in this study, the threshold is chosen such that the connectivity networks have the same density of connections (e.g., if a density of connection is set to 10%, then this means that 10% of the strongest connections in the weighted network will be assigned a value of 1 while other 90% of the connections will be assigned a value of 0). In this study, we considered binary networks with the densities of connections ranging from 5% to 100 % with increments of 5%, and we calculated network measures for each binary network formed. In addition, network measures were compared between swallowing of different fluid viscosities, as well as between swallowing in different head positions. For calculating network measures, we used the Brain Connectivity Toolbox (BCT) (Rubinov and Sporns, 2010) running on MATLAB.

- The clustering coefficient, C_i, describes the ratio between the number of existing edges which form neighborhoods around one node, and the maximum number of possible edges connecting all nodes from those neighborhoods. The formula for calculating clustering coefficient is:

$$C_i = \frac{2E_i}{D_i(D_i - 1)}, \tag{7}$$

where E_i is the number of existing edges forming neighborhoods formed around the $i - th$ node, and D_i is the degree of the i-th node. Random networks are characterized by a relatively low clustering coefficient, while networks with densely connected clusters are characterized by a high clustering coefficient (Barabási et al., 2000). The mean clustering coefficient is defined as:

$$C = \frac{1}{N}\sum_{j=1}^{N} C_j. \tag{8}$$

- Shortest path length, L_i, is the minimal number of edges connecting two nodes Strogatz (2001); Achard and Bullmore (2007), and is defined as:

$$L_{i,j} = \frac{1}{N(N-1)} \sum_{i,j \in N, i \neq j} d_{i,j}, \tag{9}$$

where $d_{i,j}$ is the shortest path length between node i and node j.

The characteristic path length is the average shortest length between all possible pairs of nodes in the graph, and is calculated as:.

$$L = \frac{1}{N}\sum_{i \in N} L_i. \tag{10}$$

- Small-worldness is characterized by a high clustering coefficient and small characteristic path length, which means that networks with small-world properties have a high formation of clustered subnetworks (Bassett and Bullmore, 2006). Two conditions describe small-world properties:

$$\gamma = \frac{C}{C_{random}} \gg 1, \tag{11}$$

and

$$\lambda = \frac{L}{L_{random}} \approx 1, \tag{12}$$

where C_{random} and L_{random} are the mean clustering coefficient and mean characteristic path of the random network, respectively. The network is said to be random if it has a low

clustering coefficient and high characteristic path length. C_{random} and L_{random} are calculated by generating many random networks for each considered network using a Markov-chain algorithm (Sporns and Zwi, 2004; Maslov and Sneppen, 2002). Small-worldness is calculated as:

$$S = \frac{C/C_{random}}{L/L_{random}}, \tag{13}$$

where the network can be said to possess small-world properties if $S > 1$.

5.5 Data analysis

For all statistical analysis we used SAS® version 9.3 (SAS Institute, Inc., Cary, North Carolina). We fit a series of linear mixed models with each of the network parameters as the dependent variable; head position, viscosity and gender, both individually and simultaneously, as fixed effect factors of interest; and a subject random effect to account for multiple measurements from the same set of participants. Appropriately constructed means contrasts were used to obtain pairwise differences. We used false discovery rate methodology to adjust the p-values for multiplicity correction. We have also measured the Cohens d effect size. Finally, we repeated the entire analysis five times, once for each of the 5 bandwidths.

Acknowledgment

Research reported in this publication was supported by the Eunice Kennedy Shriver National Institute Of Child Health & Human Development of the National Institutes of Health under Award Number R01HD074819. The content is solely the responsibility of the authors and does not necessarily represent the official views of the National Institutes of Health.

References

Achard, S., Bullmore, E., 2007. Efficiency and cost of economical brain functional networks. PLoS Computational Biology 3 (2), 174–183.

Adnerhill, I., Ekberg, O., Groher, M. E., 1989. Determining normal bolus size for thin liquids. Dysphagia 4 (1), 1–3.

Aviyente, S., Bernat, E. M., Evans, W. S., Sponheim, S. R., 2011. A phase synchrony measure for quantifying dynamic functional integration in the brain. Human Brain Mapping 32 (1), 80–93.

Aydogdu, I., Ertekin, C., Tarlaci, S., Turman, B., Kiylioglu, N., Secil, Y., 2001. Dysphagia in lateral medullary infarction (wallenbergs syndrome) an acute disconnection syndrome in premotor neurons related to swallowing activity? Stroke 32 (9), 2081–2087.

Balou, M., McCullough, G. H., Aduli, F., Brown, D., Stack Jr, B. C., Snoddy, P., Guidry, T., 2014. Manometric measures of head rotation and chin tuck in healthy participants. Dysphagia 29 (1), 25–32.

Barabási, A.-L., Albert, R., Jeong, H., 2000. Scale-free characteristics of random networks: the topology of the world-wide web. Physica A: Statistical Mechanics and its Applications 281 (1), 69–77.

Basar, E., Baar-Eroglu, C., Rahn, E., Schürmann, M., 1991. Sensory and cognitive components of brain resonance responses: an analysis of responsiveness in human and cat brain upon visual and auditory stimulation. Acta Oto-Laryngologica 111 (491), 25–35.

Baslar, E., Stampfer, H., 1985. Important associations among EEG-dynamics, event-related potentials, short-term memory and learning. International Journal of Neuroscience 26 (3-4), 161–180.

Bassett, D. S., Bullmore, E., 2006. Small-world brain networks. The Neuroscientist 12 (6), 512–523.

Bieger, D., 1993. Central nervous system control mechanisms of swallowing: a neuropharmacological perspective. Dysphagia 8 (4), 308–310.

Brown, P., Marsden, C., 1998. What do the basal ganglia do? The Lancet 351 (9118), 1801–1804.

Bülow, M., Olsson, R., Ekberg, O., 1999. Videomanometric analysis of supraglottic swallow, effortful swallow, and chin tuck in healthy volunteers. Dysphagia 14 (2), 67–72.

Choi, H.-I., Williams, W. J., 1989. Improved time-frequency representation of multicomponent signals using exponential kernels. IEEE Transactions on Acoustics, Speech and Signal Processing 37 (6), 862–871.

Clavé, P., De Kraa, M., Arreola, V., Girvent, M., Farré, R., Palomera, E., Serra-Prat, M., 2006. The effect of bolus viscosity on swallowing function in neurogenic dysphagia. Alimentary Pharmacology and Therapeutics 24 (9), 1385–1394.

Cook, I. J., Kahrilas, P. J., 1999. AGA technical review on management of oropharyngeal dysphagia. Gastroenterology 116 (2), 455–478.

Curran, J., Groher, M. E., 1990. Development and dissemination of an aspiration risk reduction diet. Dysphagia 5 (1), 6–12.

Delorme, A., Makeig, S., 2004. EEGLAB: an open source toolbox for analysis of single-trial EEG dynamics including independent component analysis. Journal of Neuroscience Methods 134 (1), 9–21.

Dodds, W. J., 1989. The physiology of swallowing. Dysphagia 3 (4), 171–178.

Donoho, D., 1995. De-noising by soft-thresholding. IEEE Transactions on Information Theory 41 (3), 613–627.

Douw, L., Schoonheim, M., Landi, D., Van der Meer, M., Geurts, J., Reijneveld, J., Klein, M., Stam, C., 2011. Cognition is related to resting-state small-world network topology: an magnetoencephalographic study. Neuroscience 175 (8), 169–177.

Eguiluz, V. M., Chialvo, D. R., Cecchi, G. A., Baliki, M., Apkarian, A. V., 2005. Scale-free brain functional networks. Physical Review Letters 94 (1), 018102.

Ertekin, C., Aydogdu, I., 2003. Neurophysiology of swallowing. Clinical Neurophysiology 114 (12), 2226–2244.

Foley, N. C., Martin, R. E., Salter, K. L., Teasell, R. W., 2009. A review of the relationship between dysphagia and malnutrition following stroke. Journal of Rehabilitation Medicine 41 (9), 707–713.

Gottlieb, D., Kipnis, M., Sister, E., Vardi, Y., Brill, S., 1996. Validation of the 50 ml3 drinking test for evaluation of post-stroke dysphagia. Disability and Rehabilitation 18 (10), 529–532.

Goyal, R. K., Padmanabhan, R., Sang, Q., 2001. Neural circuits in swallowing and abdominal vagal afferent-mediated lower esophageal sphincter relaxation. The American Journal of Medicine 111 (8), 95–105.

Hamdy, S., Mikulis, D. J., Crawley, A., Xue, S., Lau, H., Henry, S., Diamant, N. E., 1999a. Cortical activation during human volitional swallowing: an event-related fMRI study. American Journal of Physiology-Gastrointestinal and Liver Physiology 277 (1), 219–225.

Hamdy, S., Rothwell, J. C., Brooks, D. J., Bailey, D., Aziz, Q., Thompson, D. G., 1999b. Identification of the cerebral loci processing human swallowing with H2 150 PET activation. Journal of Neurophysiology 81 (4), 1917–1926.

Herrmann, C. S., Mecklinger, A., 2001. Gamma activity in human EEG is related to highspeed memory comparisons during object selective attention. Visual Cognition 8 (3-5), 593–608.

Herrmann, C. S., Sensowski, D., Röttger, S., 2004. Phase-locking and amplitude modulations of EEG alpha: Two measures reflect different cognitive processes in a working memory task. Experimental Psychology 51 (4), 311–318.

Hoffmann, S., Falkenstein, M., 2008. The correction of eye blink artefacts in the EEG: a comparison of two prominent methods. PLoS One 3 (8), 1–11.

Huckabee, M.-L., Deecke, L., Cannito, M. P., Gould, H. J., Mayr, W., 2003. Cortical control mechanisms in volitional swallowing: the bereitschaftspotential. Brain Topography 16 (1), 3–17.

Hughes, C. V., Fox, P. C., Marmary, Y., Chih-Ko Yeh, B., Sonies, B. C., 1987. Oral-pharyngeal dysphagia: a common sequela of salivary gland dysfunction. Dysphagia 1 (4), 173–177.

Hyvärinen, A., Oja, E., 2000. Independent component analysis: algorithms and applications. Neural Networks 13 (4), 411–430.

Jasper, H. H., 1958. The ten twenty electrode system of the international federation. Electroencephalography and Clinical Neurophysiology 10 (1), 371–375.

Jestrović, I., Coyle, J., Sejdić, E., 2014. The effects of increased fluid viscosity on stationary characteristics of eeg signal in healthy adults. Brain research 1589, 45–53.

Jestrović, I., Coyle, J. L., Sejdić, E., 2015. Characterizing functional connectivity patterns during saliva swallows in different head positions. Journal of NeuroEngineering and Rehabilitation 12 (1), 61–1–11.

Jestrović, I., Coyle, J. L., Sejdić, E., 2015. Decoding human swallowing via electroencephalography: a state-of-the-art review. Journal of Neural Engineering 12 (5), 051001–1–15.

Kaiser, M., Hilgetag, C. C., 2004. Edge vulnerability in neural and metabolic networks. Biological Cybernetics 90 (5), 311–317.

Kempster, G. B., 1992. Oropharyngeal swallowing in normal adults of different ages. Gastroenterology 103 (3), 823–829.

Kern, M., Birn, R., Jaradeh, S., Jesmanowicz, A., Cox, R., Hyde, J., Shaker, R., 2001. Swallow-related cerebral cortical activity maps are not specific to deglutition. American Journal of Physiology-Gastrointestinal and Liver Physiology 280 (4), 531–538.

Klemm, W., Lutes, S., Hendrix, D., Warrenburg, S., 1992. Topographical EEG maps of human responses to odors. Chemical Senses 17 (3), 347–361.

Kober, S. E., Bauernfeind, G., Woller, C., Sampl, M., Grieshofer, P., Neuper, C., Wood, G., 2015. Hemodynamic signal changes accompanying execution and imagery of swallowing in patients with dysphagia: a multiple single-case near-infrared spectroscopy study. Frontiers In Neurology 6.

Kober, S. E., Wood, G., 2014. Changes in hemodynamic signals accompanying motor imagery and motor execution of swallowing: a near-infrared spectroscopy study. Neuroimage 93, 1–10.

Kristeva-Feige, R., Feige, B., Makeig, S., Ross, B., Elbert, T., 1993. Oscillatory brain activity during a motor task. Neuroreport 4 (12), 1291–1294.

Kristeva-Feige, R., Fritsch, C., Timmer, J., Lücking, C.-H., 2002. Effects of attention and precision of exerted force on beta range EEG-EMG synchronization during a maintained motor contraction task. Clinical Neurophysiology 113 (1), 124–131.

Lago-Fernández, L. F., Huerta, R., Corbacho, F., Sigüenza, J. A., 2000. Fast response and temporal coherent oscillations in small-world networks. Physical Review Letters 84 (12), 2758–2761.

Lazarus, C., Logemann, J., 1987. Swallowing disorders in closed head trauma patients. Archives of Physical Medicine and Rehabilitation 68 (2), 79–84.

Lewin, J. S., Hebert, T. M., Putnam, J. B., DuBrow, R. A., 2001. Experience with the chin tuck maneuver in postesophagectomy aspirators. Dysphagia 16 (3), 216–219.

Logemann, J. A., 1998. The evaluation and treatment of swallowing disorders. Current Opinion in Otolaryngology and Head and Neck Surgery 6 (6), 395–400.

Logemann, J. A., Gensler, G., Robbins, J., Lindblad, A. S., Brandt, D., Hind, J. A., Kosek, S., Dikeman, K., Kazandjian, M., Gramigna, G. D., Lundy, D., McGavery-Toler, S., Miller Gardener, P., 2008. A randomized study of three interventions for aspiration of thin liquids in patients with dementia or parkinsons disease. Journal of Speech, Language, and Hearing Research 51 (1), 173–183.

Lorig, T. S., Huffman, E., DeMartino, A., DeMarco, J., 1991. The effects of low concentration odors on EEG activity and behavior. Journal of Psychophysiology 5 (1), 69–77.

Lorig, T. S., Schwartz, G. E., 1988. Brain and odor: I. alteration of human EEG by odor administration. Psychobiology 16 (3), 281–284.

Luan, B., Sörös, P., Sejdić, E., 2013. A study of brain networks associated with swallowing using graph-theoretical approaches. PloS one 8 (8), e73577.

Marik, P. E., Kaplan, D., 2003. Aspiration pneumonia and dysphagia in the elderly. CHEST Journal 124 (1), 328–336.

Martin, R. E., Goodyear, B. G., Gati, J. S., Menon, R. S., 2001. Cerebral cortical representation of automatic and volitional swallowing in humans. Journal of Neurophysiology 85 (2), 938–950.

Martin, R. E., MacIntosh, B. J., Smith, R. C., Barr, A. M., Stevens, T. K., Gati, J. S., Menon, R. S., 2004. Cerebral areas processing swallowing and tongue movement are overlapping but distinct: a functional magnetic resonance imaging study. Journal of Neurophysiology 92 (4), 2428–2493.

Martin, R. E., Sessle, B. J., 1993. The role of the cerebral cortex in swallowing. Dysphagia 8 (3), 195–202.

Maslov, S., Sneppen, K., 2002. Specificity and stability in topology of protein networks. Science 296 (5569), 910–913.

Masuda, N., Aihara, K., 2004. Global and local synchrony of coupled neurons in small-world networks. Biological Cybernetics 90 (4), 302–309.

Mathewson, K. E., Lleras, A., Beck, D. M., Fabiani, M., Ro, T., Gratton, G., 2011. Pulsed out of awareness: EEG alpha oscillations represent a pulsed-inhibition of ongoing cortical processing. Frontiers in Psychology 2 (1).

Mcconnel, F., 1988. Analysis of pressure generation and bolus transit during pharyngeal swallowing. The Laryngoscope 98 (1), 71–78.

Micheloyannis, S., Pachou, E., Stam, C. J., Vourkas, M., Erimaki, S., Tsirka, V., 2006. Using graph theoretical analysis of multi channel EEG to evaluate the neural efficiency hypothesis. Neuroscience Letters 402 (3), 273–277.

Miller, A. J., 1986. Neurophysiological basis of swallowing. Dysphagia 1 (2), 91–100.

Miller, A. J., 1999. The neuroscientific principles of swallowing and dysphagia. Singular Publishing Group San Diego, San Diego, CA.

Miller, J. L., Watkin, K. L., 1996. The influence of bolus volume and viscosity on anterior lingual force during the oral stage of swallowing. Dysphagia 11 (2), 117–124.

Mosier, K., Bereznaya, I., 2001. Parallel cortical networks for volitional control of swallowing in humans. Experimental Brain Research 140 (3), 280–289.

Murray, J., 1999. Manual of dysphagia assessment in adults. Singular, San Diego, CA.

Nicosia, M. A., Robbins, J., 2001. The fluid mechanics of bolus ejection from the oral cavity. Journal of Biomechanics 34 (12), 1537–1544.

Niedermeyer, E., da Silva, F. L., 2005. Electroencephalography: basic principles, clinical applications, and related fields. Lippincott Williams & Wilkins, Philadelphia, PA.

Olbrich, S., Jödicke, J., Sander, C., Himmerich, H., Hegerl, U., 2011. ICA-based muscle artefact correction of EEG data: What is muscle and what is brain?: Comment on mcmenamin et al. Neuroimage 54 (1), 1–3.

Reimers-Neils, L., Logemann, J., Larson, C., 1994. Viscosity effects on EMG activity in normal swallow. Dysphagia 9 (2), 101–106.

Rogers, B., Arvedson, J., Buck, G., Smart, P., Msall, M., 1994. Characteristics of dysphagia in children with cerebral palsy. Dysphagia 9 (1), 69–73.

Rubinov, M., Sporns, O., 2010. Complex network measures of brain connectivity: uses and interpretations. Neuroimage 52 (3), 1059–1069.

Saitoh, E., Shibata, S., Matsuo, K., Baba, M., Fujii, W., Palmer, J. B., 2007. Chewing and food consistency: effects on bolus transport and swallow initiation. Dysphagia 22 (2), 100–107.

Sanes, J. N., Donoghue, J. P., 1993. Oscillations in local field potentials of the primate motor cortex during voluntary movement. Proceedings of the National Academy of Sciences 90 (10), 4470–4474.

Sang, Q., Goyal, R. K., 2001. Swallowing reflex and brain stem neurons activated by superior laryngeal nerve stimulation in the mouse. American Journal of Physiology-Gastrointestinal and Liver Physiology 280 (2), 191–200.

Satow, T., Ikeda, A., Yamamoto, J.-i., Begum, T., Thuy, D. H. D., Matsuhashi, M., Mima, T., Nagamine, T., Baba, K., Mihara, T., et al., 2004. Role of primary sensorimotor cortex and supplementary motor area in volitional swallowing: a movement-related cortical potential study. American Journal of Physiology-Gastrointestinal and Liver Physiology 287 (2), 459–470.

Sauseng, P., Klimesch, W., Doppelmayr, M., Pecherstorfer, T., Freunberger, R., Hanslmayr, S., 2005. EEG alpha synchronization and functional coupling during top-down processing in a working memory task. Human Brain Mapping 26 (2), 148–155.

Sejdić, E., Komisar, V., Steele, C., Chau, T., 2010. Baseline characteristics of dual-axis cervical accelerometry signals. Annals of Biomedical Engineering 38 (3), 1048–1059.

Sejdić, E., Steele, C., Chau, T., 2009. Segmentation of dual-axis swallowing accelerometry signals in healthy subjects with analysis of anthropometric effects on duration of swallowing activities. IEEE Transactions on Biomedical Engineering 56 (4), 1090–1097.

Sejdić, E., Steele, C., Chau, T., 2012. A method for removal of low frequency components associated with head movements from dual-axis swallowing accelerometry signals. PLoS One 7 (3), 33464–33473.

Shaker, R., Cook, I. J., Dodds, W. J., Hogan, W. J., 1988. Pressure-flow dynamics of the oral phase of swallowing. Dysphagia 3 (2), 79–84.

Shanahan, T. K., Logemann, J. A., Rademaker, A. W., Roa Pauloski, B., 1993. Chin-down posture effect on aspiration in dysphagic patients. Archives of Physical Medicine and Rehabilitation 74 (7), 736–739.

Smithard, D., O'neill, P., Park, C., Morris, J., Wyatt, R., England, R., Martin, D., 1996. Complications and outcome after acute stroke. Does dysphagia matter? Stroke 27 (7), 1200–1204.

Sporns, O., Zwi, J. D., 2004. The small world of the cerebral cortex. Neuroinformatics 2 (2), 145–162.

Srivastava, G., Crottaz-Herbette, S., Lau, K., Glover, G., Menon, V., 2005. ICA-based procedures for removing ballistocardiogram artifacts from EEG data acquired in the MRI scanner. Neuroimage 24 (1), 50–60.

Stacher, G., Bauer, H., Steinringer, H., 1979. Cholecystokinin decreases appetite and activation evoked by stimuli arising from the preparation of a meal in man. Physiology & Behavior 23 (2), 325–331.

Stevenson, R. D., Allaire, J. H., 1991. The development of normal feeding and swallowing. Pediatric Clinics of North America 38 (6), 1439–1453.

Strogatz, S. H., 2001. Exploring complex networks. Nature 410 (6825), 268–276.

Urigüen, J. A., Garcia-Zapirain, B., 2015. EEG artifact removalstate-of-the-art and guidelines. Journal of Neural Engineering 12 (3), 1–23.

Watts, D. J., Strogatz, S. H., 1998. Collective dynamics of small-world networks. Nature 393 (6684), 440–442.

Welch, M. V., Logemann, J. A., Rademaker, A. W., Kahrilas, P. J., 1993. Changes in pharyngeal dimensions effected by chin tuck. Archives of Physical Medicine and Rehabilitation 74 (2), 178–181.

Yagyu, T., Kondakor, I., Kochi, K., Koenig, T., Lehmann, D., Kinoshita, T., Hirota, T., Yagyu, T., 1998. Smell and taste of chewing gum affect frequency domain EEG source localizations. International Journal of Neuroscience 93 (3-4), 205–216.

Yang, H., Guan, C., Chua, K. S. G., Wang, C. C., Soon, P. K., Tang, C. K. Y., Ang, K. K., 2014. Detection of motor imagery of swallow eeg signals based on the dual-tree complex wavelet transform and adaptive model selection. Journal of Neural Engineering 11 (3), 035016.

Yang, H., Guan, C., Wang, C. C., Ang, K. K., Phua, K. S., San Chok, S., Tang, C. K. Y., Chua, K. S. G., 2016. On the correlations of motor imagery of swallow with motor imagery of tongue movements and actual swallow. In: Advances in Cognitive Neurodynamics (V). Springer, pp. 397–404.

Yordanova, J., Kolev, V., Rosso, O. A., Schürmann, M., Sakowitz, O. W., Özgören, M., Basar, E., 2002. Wavelet entropy analysis of event-related potentials indicates modality-independent theta dominance. Journal of Neuroscience Methods 117 (1), 99–109.

Zald, D. H., Pardo, J. V., 1999. The functional neuroanatomy of voluntary swallowing. Annals of Neurology 46 (3), 281–286.

Figure legends

Figure 1 - The value of mean clustering coefficient, C, for different threshold percentages and for different frequency bands, of three liquid viscosities swallows in the 5 EEG frequency bands. Each colored line indicates a mean value and standard deviation for the clustering coefficient of various bolus viscosity. A ring shows the density of the connection where is significant statistical difference between water and nectar, a rhomb shows density of the connection where there is significant statistical difference between water and honey, while solid circle shows the density of the connection where is significant statistical difference between nectar and honey.

Figure 2 - The value of mean characteristic path length, L, for different threshold percentages and for different frequency bands, of three liquid viscosities swallows in the 5 EEG frequency bands. Each colored line indicates a mean value and standard deviation for the clustering coefficient of various bolus viscosity. A ring shows the density of the connection where is significant statistical difference between water and nectar, a rhomb shows density of the connection where there is significant statistical difference between water and honey, while solid circle shows the density of the connection where is significant statistical difference between nectar and honey.

Figure 3 - The value of mean small-worldness, S, for different threshold percentages and for different frequency bands, of three liquid viscosities swallows in the 5 EEG frequency bands. Each colored line indicates a mean value and standard deviation for the clustering coefficient of various bolus viscosity. A ring shows the density of the connection where is significant statistical difference between water and nectar, a rhomb shows density of the connection where there is significant statistical difference between water and honey, while solid circle shows the density of the connection where is significant statistical difference between nectar and honey.

Figure 4 - Average connectivity brain networks with the 25% of the strongest connections in various conditions.

Figures

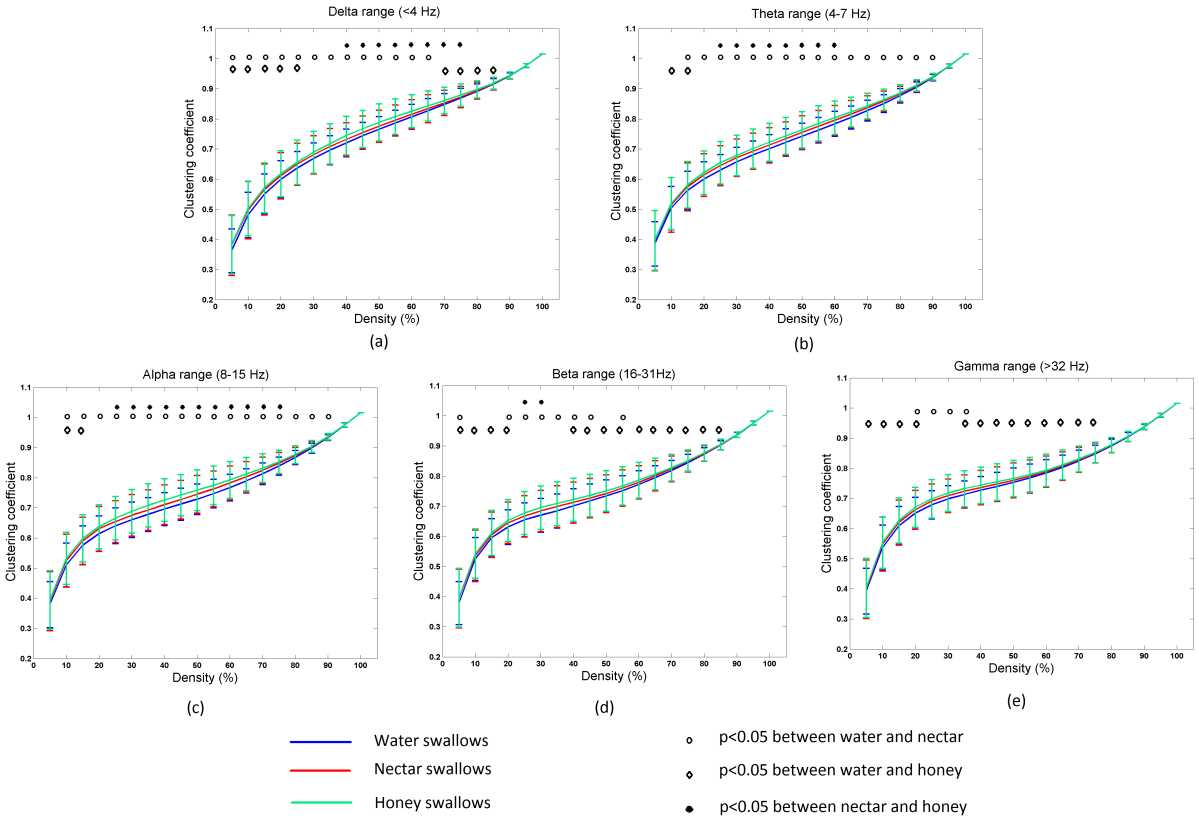

Figure 1:

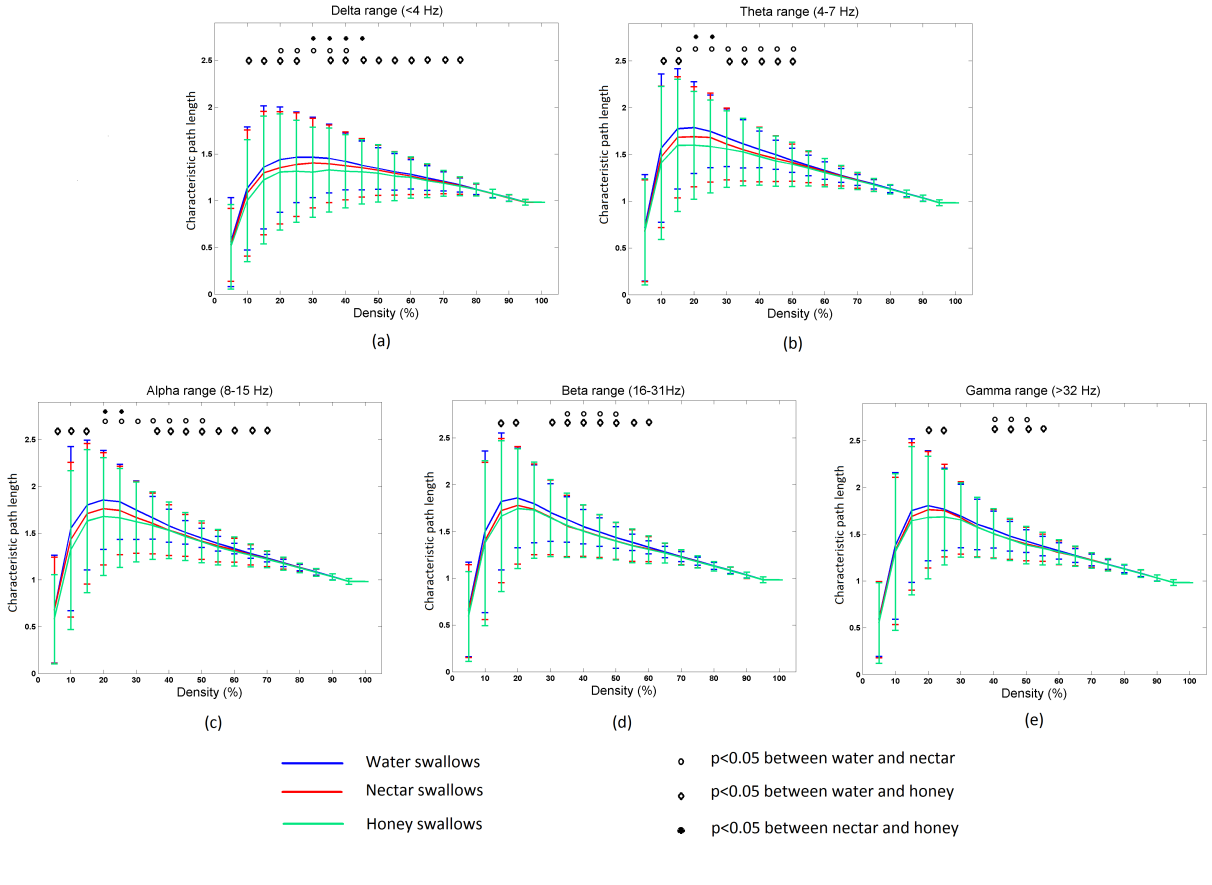
Delta range (<4 Hz)
Theta range (4-7 Hz)
Alpha range (8-15 Hz)
Beta range (16-31Hz)
Gamma range (>32 Hz)
Characteristic path length
Density (%)
(a)
(b)
(c)
(d)
(e)
Water swallows
Nectar swallows
Honey swallows
p<0.05 between water and nectar
p<0.05 between water and honey
p<0.05 between nectar and honey

Figure 2:

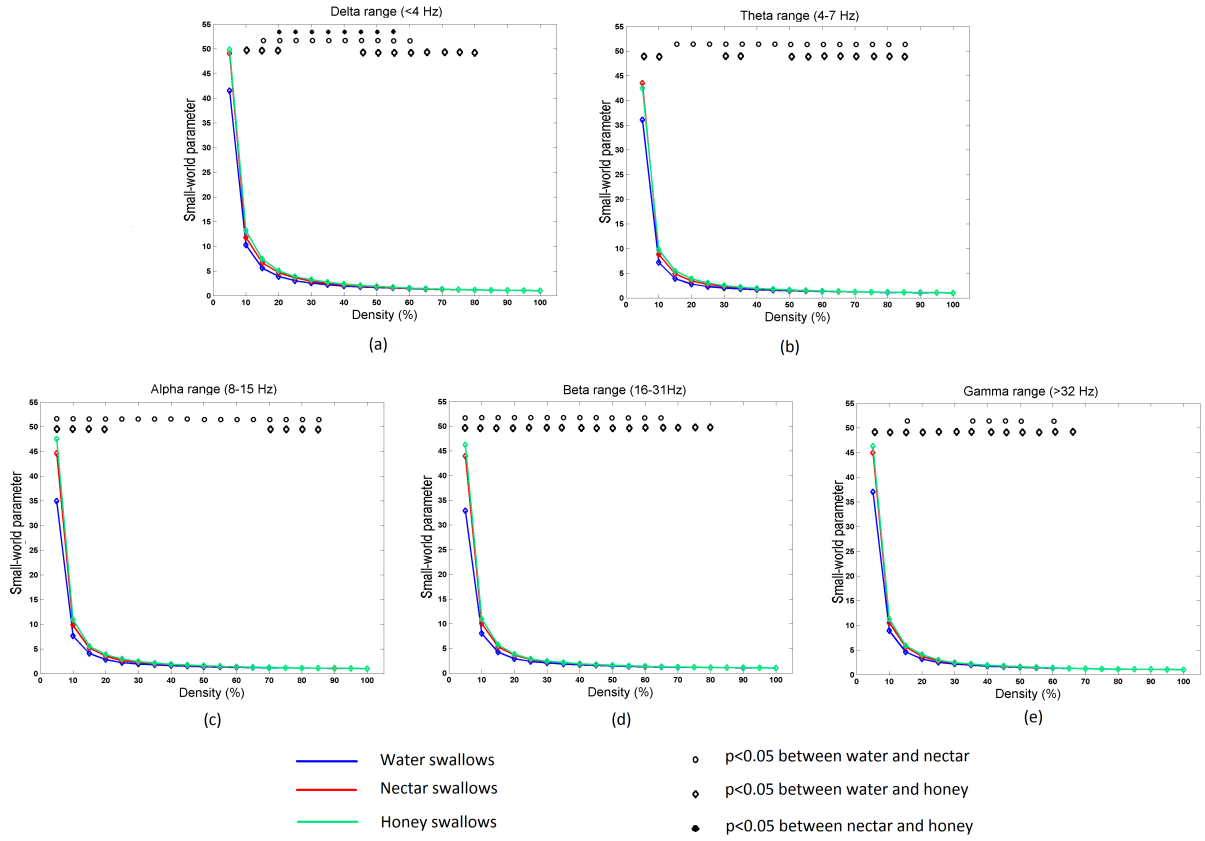
Delta range (<4 Hz)
Theta range (4-7 Hz)
Alpha range (8-15 Hz)
Beta range (16-31Hz)
Gamma range (>32 Hz)
Small-world parameter
Density (%)
(a)
(b)
(c)
(d)
(e)
Water swallows
Nectar swallows
Honey swallows
p<0.05 between water and nectar
p<0.05 between water and honey
p<0.05 between nectar and honey

Figure 3:

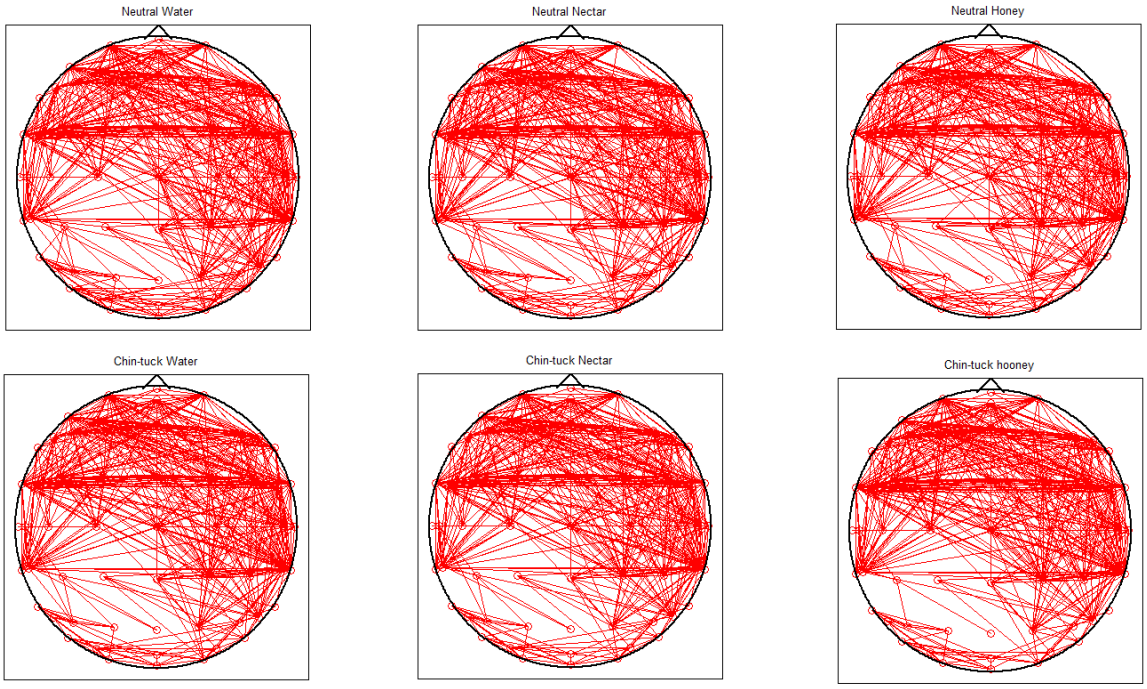
Neutral Water
Neutral Nectar
Neutral Honey
Chin-tuck Water
Chin-tuck Nectar
Chin-tuck hooney

Figure 4: